Characterization of Ambient Particulate Matter Sampled at an Active Sand Mine Facility in Northwestern Wisconsin

Julie Zhang,[1,2] Callie Fischer,[1] Joe Oster,[1] Gabriel de Carvalho Chaves,[1,3] Rachel Mooney,[1] & Patricia Cleary[1]*

[1]Department of Chemistry, University of Wisconsin - Eau Claire, Eau Claire, WI
[2]now at University of Wisconsin-Madison, Madison, WI
[3]now at Pontifícia Universidade Católica de Minas Gerais, Brazil

Students: jzhang555@wisc.edu[*], fischerca@uwec.edu, joester93@hotmail.com, gabrielcarch@gmail.com, mooney.rachel23@gmail.com
Mentor: clearypa@uwec.edu[*]

ABSTRACT

Concern has arisen about levels of silica in ambient particles near sand mines in Northwestern Wisconsin. Airborne particles released from mining and processing activity may release respirable silica into the air, which can have adverse health effects on individuals exposed to significant quantities. In order to assess these levels of silica, this study developed a parallel analysis using an X-ray diffraction (XRD) and scanning electron microscopy/energy-dispersive X-ray spectroscopy (SEM-EDS) analysis to test particles in real air samples. Calibrations were constructed for the XRD analysis (following NIOSH Method 7500) with silica standards containing 10 μg – 500 μg respirable silica on filter media with detection limits of 19-28 μg. SEM-EDS methods incorporated identifying the geologic composition of particles using the elemental analysis. Real air samples were collected at a sand mining site using a cascade impactor. Filter substrates were pre-weighed and post-weighed to determine the total dry mass of particles sampled and XRD results show at maximum 16 % of the mass can be attributed to crystalline silica in the samples. An SEM-EDS analysis to categorize the particles geologic classification using ratios of elements shows more than 70% of sampled particles are classified as potassium feldspars.

KEYWORDS

Particulate Matter; Sand Mining; Silica; Atmospheric Characterization; XRD; SEM-EDS; Fugitive Dust

INTRODUCTION

Airborne particulate matter is a highly variable and complex mixture of solid or liquid matter. Both natural and anthropogenic sources are responsible for the distribution of primary particulate matter in air. Particles with the potential to cause health effects are associated with its size, composition, and concentration in the air, where typical federal regulations identify hazards by particle size and concentration.[1] Particulate matter composed of crystalline silica poses a health threat.[2] Emission of silica-containing particulate matter may occur during sand mining in Wisconsin as sandstone is crushed and broken apart, releasing dust particles into the air.[3] The sand mining industry has grown immensely in Wisconsin in the past years, from just 8 industrial sand facilities in 2008 to 129 in 2015, making Wisconsin the nation's leading sand producer due to the demand for specialized sand used in hydrofracking operations (referred to as frac sand mining).[4] As the number of frac sand mining facilities in Wisconsin increased rapidly, concern has arisen on the correlation between the sand mining boom and the potential for increasing ambient particle concentrations which may contain respirable crystalline silica. Residents near the frac sand sites have concerns about the potential exposure to respirable crystalline silica in the air. With no federal or state guidelines or standards for respirable crystalline silica in ambient air, Minnesota Department of Health and California Office of Environmental Health Hazarded Assessments established an air quality chronic health-based value (HBV) of 3.0 μg/m^{3} for respirable crystalline silica.[5]

Silica, silicon dioxide (SiO_2), is one of the most abundant compounds in Earth's crust being present in most of the rocks and soils. It is found with both amorphous microstructure and crystalline structure, and three principal forms: quartz, cristobalite, and tridymite. Crystalline silica particles, primarily quartz dust, are known to be a human carcinogen.[6] Respirable crystalline silica is defined as silicon dioxide particulates of 4 micrometers or less in diameter (PM_4) by OSHA.[7] Excess exposure to these particles can lead to the development of silicosis, airway diseases, pulmonary tuberculosis, chronic renal disease, and lung cancer.[1] PM_{10} silica particles can become airborne and be inhaled and enter the lungs. Particles of a diameter of 4 μm or less pose a greater health hazard. Not only are these particles small enough to enter the lungs, but they can also travel into the alveolar regions of the lungs where they can cause irreparable damage.[8] Alveolar macrophages engulf but fail to dissolve the particles, triggering an inflammatory response.[9] The scar tissue left by this damage can, over time, result in the production of shortness of breath, poor gas exchange in the lungs, fatigue, and in extreme cases, respiratory failure.

The Occupational Safety and Health Administration established a Reference Exposure Limit (REL) for respirable crystalline silica at 50 μg/m^{3} averaged over an 8-hour working shift.[10] The recommended analysis, NIOSH method 7500,[7] uses XRD analysis to determine silica concentrations. This method aims to collect atmospheric particles with the use of polycarbonate filters and cyclones samplers. Samples are prepared by ashing the filters and depositing the resulting ash onto silver filters, which are then

analyzed by XRD. NIOSH Method 7500 has been used by Sanderson *et al.* to evaluate respirable silica abundance near sand mines.[2] Other studies that utilize the NIOSH method to measure respirable silica include Shiraki *et al.*'s study[11] on silica exposure near a sand facility in central California, and Richards *et al.* studies[12, 13] at Aggregate-Producing-sources in California and at frac sand mining facilities in Wisconsin.

The sandstone material being mined in western Wisconsin consists mainly of well-rounded quartz grains (95%), a majority in the 0.3-0.6 mm diameter range, ideal for use in hydraulic fracking operations[14]. The interstitial spaces consist of void spaces and cement made up of dolomite, hematite, authigenic potassium feldspar, illite, and authigenic quartz, based on a previous study on the Wowenoc and Jordan formations.[15] The components of the cement pose no added health concern for their composition in particulate matter. Due to the history of crystalline silica particle emissions from sand mining,[2] this study is aimed at investigating the amount of quartz found in ambient particles emitted at these mines.

Two studies have investigated particles in areas near to frac sand mines in Wisconsin. Walters *et al.* investigated $PM_{2.5}$ airborne particulates near frac sand operations using an SKC DPS sampler to determine $PM_{2.5}$ concentrations.[3] Authors of this study assumed that all the $PM_{2.5}$ particles counted were silica, concluding that there is an increase of ambient $PM_{2.5}$ levels as a result of increasing frac sand mining. On the other hand, another study by John Richards at EOG facilities monitored air emissions for crystalline silica at PM_4 and collected 657 average daily measurements from the fence lines of sand producing facilities in Wisconsin.[13] The study described measurements of local $PM_{2.5}$ monitoring stations as representing regional fine particle loading, and the results showed there is little influence by nearby sand mine operations. NIOSH Method 7500 was followed, sample values below the limit of quantification were treated as zeros, XRD results showed the average long-term ambient PM_4 crystalline silica concentrations ranged between 0.05 and 0.45 $\mu g/m^3$, from 5% to 20% of the Minnesota Department of Health's and California Office of Environmental Health Hazarded Assessments' exposure level of 3.0 $\mu g/m^3$. However, this study only measured the concentration of crystalline silica at PM_4, and the composition of the particles that were not silica remained unresolved.

One way to solve the discrepancy between these two studies is to conduct some elemental analysis on the sampled particles using SEM-EDS. This strategy has been employed successfully by many groups to develop parameters for principal component analysis and source apportionment.[16-18] Moreno *et al.*[19] used scanning electron microscopy-energy dispersive spectroscopy in order to characterize the geology of ambient particles. Many others have used multi-instrumentation approaches to characterize ambient particles and their sources better.[20, 21]

To have a better understanding of both the levels of crystalline silica and elemental composition of particles in the air, this study quantitatively and qualitatively measured respirable particles near frac sand mining sites in Wisconsin. Because of the toxicity of respirable crystalline silica, the analysis focuses on the identification of quartz with respect to other materials in the particles. Scanning electron microscopy-energy dispersive spectroscopy (SEM-EDS) and X-ray diffraction (XRD), were used to directly test for crystalline silica and other geologic parent material using elemental analysis. Samples for XRD analysis were prepared based on a modified version of NIOSH method 7500.

METHODS AND PROCEDURES

Sample Collection

Samples were collected using two Sioutas Personal Cascade Impactors, each composed of four stages, used to separate particulate matter based on size. Using the Leland Legacy Sample Pumps at a flow rate of 9 L/min for 24 hours, filters were sampled at the Fairmont Santrol mine in Menomonie, WI next to the "Grizzly," a rock crusher with no fugitive dust control measures in an open area. Typically the machine was operated in either 2 or 3 shifts (16 to 24 hours a day). The cascade impactors were each loaded with four pre-weighed 25 mm diameter 2.0 µm pore size filters made of polycarbonate (for XRD analysis) or PTFE (for SEM-EDS analysis). Airborne particles were separated into four size ranges: >2.5 µm, 1.0-2.5 µm, 0.50-1.0 µm, and 0.25-0.50 µm, corresponding to stages A, B, C, and D respectively. An identical field blank filter was used as a control for comparison. Each set of samples was collected for 24 hours. Pre- and post-weighing of desiccated filters to the nearest 0.01 mg was performed to determine deposited particle mass. The weighing process was performed a minimum of three times until a variability of less than 0.1% was achieved.

Sampling Date	SEM analysis	XRD analysis	Gravimetric
6/25/15	X		
7/27/15	X	X	
9/24/15	X	X	X
11/15		X	X

Table 1: Overall sampling at Menomonie site with two particle samplers equipped with filters for either SEM or XRD analysis. Gravimetric analysis was conducted on filters used for XRD analysis that were pre-weighed before sampling.

XRD Analysis

The quartz component of the particles has significant health implications, so the XRD analysis focused exclusively on the identifying the amount of crystalline silica collected. Sample preparation for analysis by X-ray diffraction was performed using a modified version of NIOSH Method 7500. Polycarbonate and silica standard filters were ashed in a muffle furnace at 500°C for 2 hours. The ash was then suspended in 2-propanol, and the suspension was subjected to an ultrasonic bath for 30 minutes to break up agglomerated particles. Particles were deposited onto a silver filter using a vacuum filtration apparatus. The filters were heat-fixed to a glass slide using Parlodion solution and mounted on the XRD (Bruker D8 Discover).

A calibration curve for the XRD analysis method was constructed using 10 µg, 20 µg, 50 µg, 100 µg, 250 µg and 500 µg silica calibration standard filters from NIST's Standard Reference Material division. Filters were subjected to the sample preparation method and analyzed by XRD. Peak areas were measured versus quartz masses to derive a linear equation. The detection limit, DL, was calculated as:

$$DL = 3s_x/m$$ **Equation 1.**

where s_x is the standard deviation of the intercept, and *m* is the slope of the linear calibration curve generated. Two calibrations were made on July 25, 2015, and June 6, 2016. The equation derived from the standard calibration curve was used to solve for quartz mass in the three samples from the field using the peak areas obtained from the sample XRD spectra.

Full XRD rotation was used to ensure use of continuous angles of a sample to help eliminate random errors that may occur when repeatedly testing multiple fixed angles. Peak areas were measured from the peak maximum at 26.66° (2θ) to ± 4*width to calculate the tails range for each peak (**Figure 1**). Due to the time-intensive nature of the XRD scans (~5 hours each) and the small sample material amounts, the XRD was only used to quantify quartz.
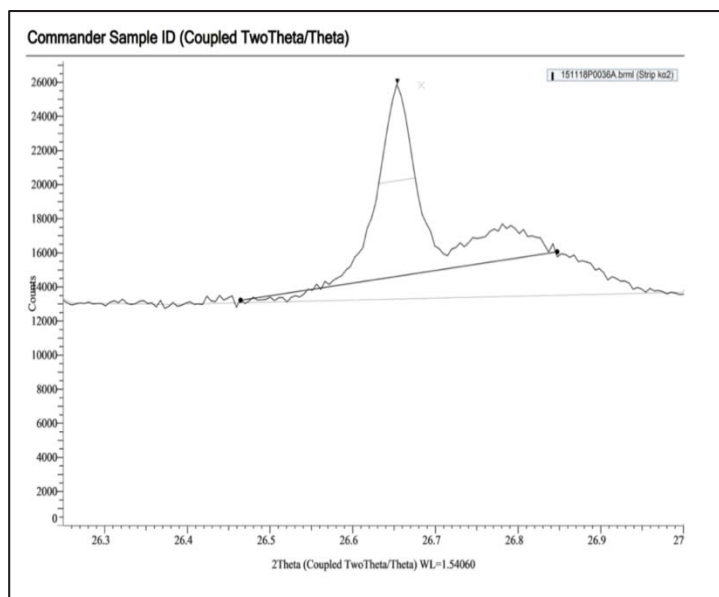

Figure 1. Area under the primary peak of quartz at 26.66 °2θ was calculated using XRD.

SEM-EDS Analysis

Elemental characterization of the particles was done using a scanning electron microscope. Particles from the sample were transferred onto carbon tape which was placed on an aluminum stub. The particles were analyzed using scanning electron microscopy (Hitachi S-3400N Variable Pressure SEM) coupled with energy dispersive spectroscopy (EDS with ~ 1-micron resolution). The microscope working distance was 10 mm with an accelerating voltage of 15 kV and had an acquisition of 60 s live time. The X-ray point-and-shoot and linescan methods were used to run the analysis. The point and shoot method focused on a specific point on a particle, providing an elemental analysis of a particular spot (See **Figure 2**). The sample was broken up into three zones and six sections. A random number generator was used to select one of these sections to analyze, and this process was repeated 6 times per filter. The points analyzed formed a grid of six points, three on top and three below per section totaling N=36 for each filter stage (if sufficient particles were available). The point-and-shoot analysis can only perform this analysis on an area down to 0.5 µm in diameter, so this method was only used for elemental analysis of the largest particulate sample, stage A.

The linescan method was used to analyze the other three stages, B-D on 9/24/15. Rather than analyzing individual points, the linescan method analyzes 100 points along a line to produce a spectrum, allowing a larger sample of particles to be

analyzed per each section. Each filter sample produced 1200 data points. In the linescan method, the sample was broken up into five zones and each zone into six sections. Like the point-and-shoot method, one of the six sections was selected for analysis using a random number generator. Four linescans were run in the shape of a pound sign to analyze multiple particles in the sample. This process was repeated for each of the five zones. The data collected was categorized into different geological classes, which was modified from the analysis outlined in Moreno *et al.*[19] using determined atom percent (**Table 2**).

Composition label	Identifying factor	Al#= Al/SUM	Mg#= Mg/SUM	(Mg+Fe)#= (Mg+Fe)/SUM	Al/Si	Si#= Si/SUM
Other	Large other elemental component					
Illite	Mg+Fe>5% SUM					
Hematite	Fe >5% SUM					
K-Feldspar		Al#<25	Mg#<25	(Mg+Fe) #<25	Al/Si>0.2	Si#>50
Quartz	Si dominant (SUM – Si< 10%)	Al#<25	Mg#<25	(Mg+Fe) #<25	Al/Si<0.2	Si#>50
Diesel	Sulfur atom % > 5%					

Table 2. Classification scheme for SEM-EDS analysis. The inputs are the atom percent of Al, Mg, Si, and Fe, where SUM = (Al+Mg+Fe+Si+K).
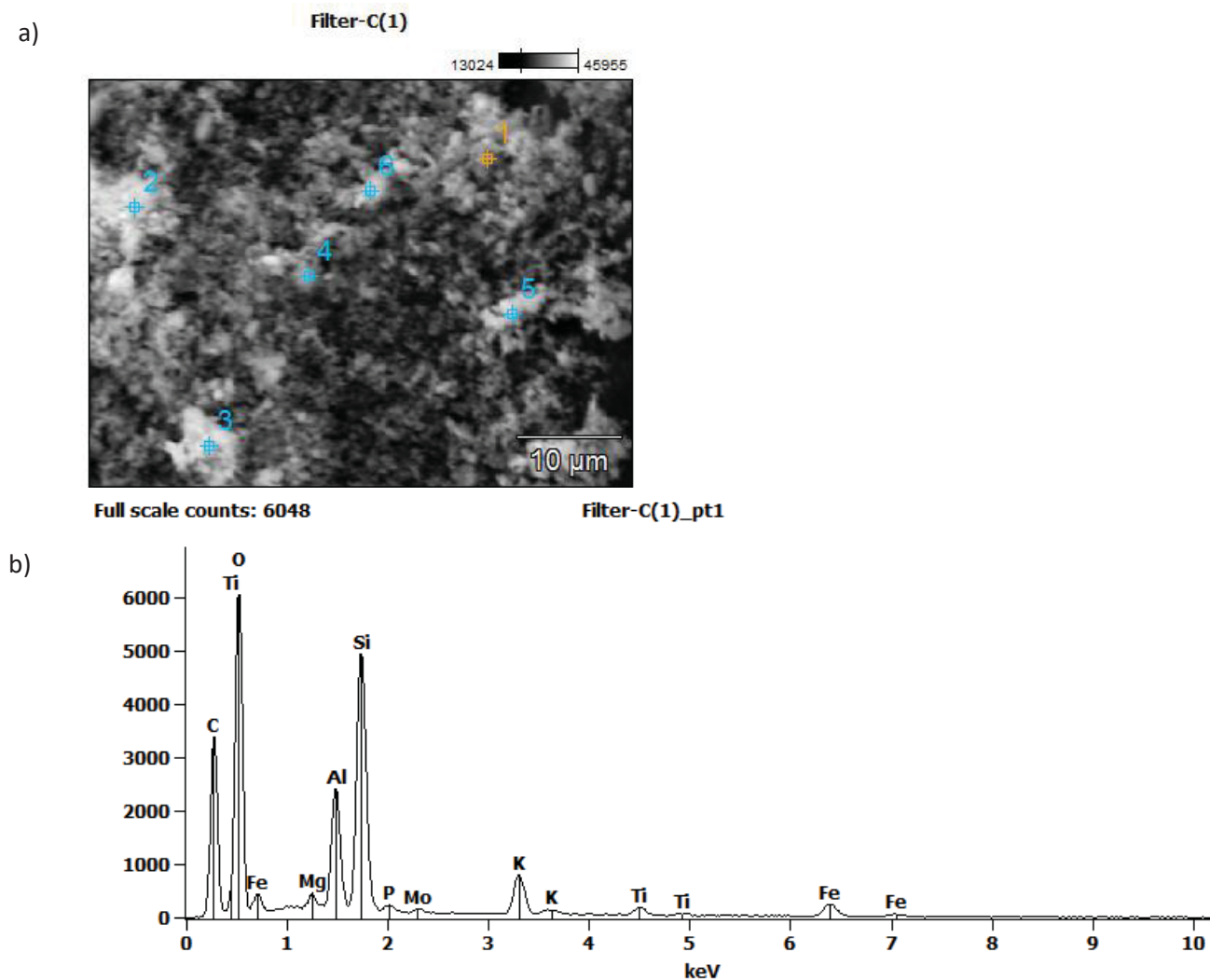

Figure 2. Example SEM image (a) of Stage C sample from 7/27/17 with EDS spectrum b) from Point 1.

RESULTS

Four 24-hour samples were analyzed over the summer and fall of 2015, but not all analysis types were able to be conducted for all sampling days (**Table 1**). A calibration graph for XRD was made on June 6, 2016 gave a detection limit (DL) of 19μg, with y = 0.00713 (± 0.00018) x - 0.007 (± 0.044). Particle mass deposited on the sample filters in the 2.5-10 μm diameter group range from 250 to 1300 μg. Silica peak areas on the XRD were relatively small, requiring long time-averaged scans of 4-5 hours, with estimate quartz mass between 4-63 μg. The nearest in time calibration curve was applied to each set of samples to process the data. Many samples were below the XRD detection limit for quartz. When above the detection limit, the percent quartz of the particle mass deposited on the filters was 16%. **Table 3** shows reported results for XRD analysis and gravimetric analysis. The particle concentration in the air was calculated from the particle mass, the 24-hour sampling period and the flow rate of the pump used with the cascade impactor (9 Liters per minute). The quartz concentration in the air was calculated similarly but starting with the calculated quartz mass from the XRD analysis.

Results from 7/27/2015 had a detection limit of 28 μg. The decrease in silica net peak areas indicates smaller particle size and fewer particles collected on the filters. The calculated quartz mass from the particle size range of 2.5-10 μm was 63 μg. Pre-weights of filters were not measured. Therefore, overall particle mass deposited on filter and quartz percent on filters were unable to be obtained. Calculated quartz concentration in the air was 4.9 μg/m³ for particle size 2.5-10μm, and 2.2 μg/m³ for particle size 1.0-2.5μm. Results from Sept. 24, 2015, had a detection limit of 28 μg. Quartz mass from the particle size range of 2.5-10 μm is 39 μg, about 16% of the total particles collected on the filters. The calculated concentration of quartz in the air was 2 μg/m³. Results from 11/2015 had a detection limit of 19 μg. Estimate quartz masses were all below the detection limit. It is noted that there were significant amounts of particles deposited on filters, ranging from 1330 μg for particle size 2.5-10 μm, to 330 μg for particle size 0.25-0.5 μm.

Cascade Impactor Stages (particle aerodynamic diameters)	XRD quartz peak net area (counts × degrees)	Calculated quartz mass (μg)	Particle mass deposited on filters (μg)	% Quartz on Filters	Particle concentration in the air (μg/m³)	Quartz concentration in the air (μg/m³)
Sample Date: 07/27/2015						
A (2.5-10 μm)	0.3736	63	-	-	-	4.9
B (1.0-2.5 μm)	0.1007	28	-	-	-	2.2
C (0.50-1.0 μm)	0.08242	< DL	-	-	-	-
D (0.25-0.5 μm)	0.03213	< DL	-	-	-	-
Blank	0.01325	< DL	-	-	-	-
Sample Date: 09/24/2015						
A (2.5-10 μm)	0.1951	39	250	16%	19	3.0
B (1.0-2.5 μm)	0.04110	< DL	70	-	5	-
C (0.50-1.0 μm)	-	-	-	-	-	-
D (0.25-0.5 μm)	0.002000	< DL	50	-	4	-
Blank	-	-	-	-	-	-
Sample Date: 11/2015						
A (2.5-10 μm)	0.02115	< DL	1330	-	103	-
B (1.0-2.5 μm)	0.01126	< DL	560	-	43	-
C (0.50-1.0 μm)	0.008146	< DL	330	-	25	-
D (0.25-0.5 μm)	0.006028	< DL	330	-	25	-
Blank	-	-	-	-	-	-

Table 3. Particle mass, XRD Data and Calculated Values for polycarbonate filters.

SEM-EDS analysis determined the particle composition of the samples. The main elements found in all samples were, in decreasing order, oxygen (53.8%), silicon (23.2%), aluminum (9.3%), potassium (5.8%), iron (3.4%) and magnesium (1.4%). The sum of atom percent of all elements excluding carbon was from 58-99% for all samples. Carbon was excluded from the analysis due to interference from the carbon tape used in the SEM analysis (blank scans on the SEM-EDS show carbon as the main

element). Samples with the highest amount of carbon were samples with fewer particles transferred to the carbon tape, consistent with the assumption that the carbon signal is background.

Particles were placed into five categories: potassium feldspar (abbreviated as kspar), quartz, hematite, illite, diesel and other based on their elemental composition. The identifying characteristics sorted based atom percent of elements, was established from both SEM-EDS analysis of thin-film sections of the Jordan formation with geologic identification from previous work,[15] samples of pure quartz, calcite, hematite, diesel particles and modifications of the analysis established in Moreno *et al*.[19] (See **Table 2**). For all sampling dates, the majority of sampled particles were classified as potassium feldspars (see **Table 4**), which could also be considered kaolinite clays based on the depositional history of the formation.[15] The composition varies slightly for cements that have some characteristics of hematite (high iron content). While we classify these as hematite, the identifying signature is being iron-rich based on the other elements observed.

	Kspar	**Hematite**	**Illite**	**Quartz**	**Other**
6/25/15					
A (2.5-10 μm)	94.44%	0.00	0.00	5.56	0.00
B (1.0-2.5 μm)	86.67	5.00	0.00	1.67	6.67
C (0.50-1.0 μm)	90.00	6.67	0.00	0.00	3.33
D (0.25-0.5 μm)	80.00	13.33	0.00	3.33	3.33
7/27/15					
A (2.5-10 μm)	70.00	23.33	0.00	0.00	6.67
B (1.0-2.5 μm)	53.33	43.33	0.00	3.33	0.00
C (0.50-1.0 μm)	86.67	10.00	0.00	0.00	0.00
D (0.25-0.5 μm)	76.67	23.33	0.00	0.00	0.00
9/24/15					
A (2.5-10 μm)	61.11	33.33	0.00	2.78	2.78
B (1.0-2.5 μm)	95.20	3.65	0.09	0.00	1.07
C (0.50-1.0 μm)	96.85	2.04	0.00	0.00	1.11
D (0.25-0.5 μm)	49.94	49.94	0.00	0.00	0.13

Table 4 Geologic composition of Teflon filter set sampled on 6/25/2015, 7/27/15, and 9/27/15 using SEM-EDS elemental analysis.

The largest particle size (Stage A) typically has more identifiable different particle categories, perhaps due to the more precise point-and-shoot sampling technique. However, it should be noted that for most of the particles sampled, some component can be attributed to quartz for almost all filter stages, but not necessarily uniformly. **Figure 3** shows the overall average composition of all samples, of which 2.5% are classified as quartz using SEM-EDS. The percent of quartz particles in each filter stage was between 0.00 and 7.41% of the total particles. The ambient particles were mainly potassium feldspars (78.4%), secondarily hematite (17.8%), with small amounts of quartz (2.1%). The "other" category corresponds to particles that were unidentifiable, some of which contained large amounts of phosphorus, and trace amounts of transition metals such as titanium, molybdenum, and scandium.
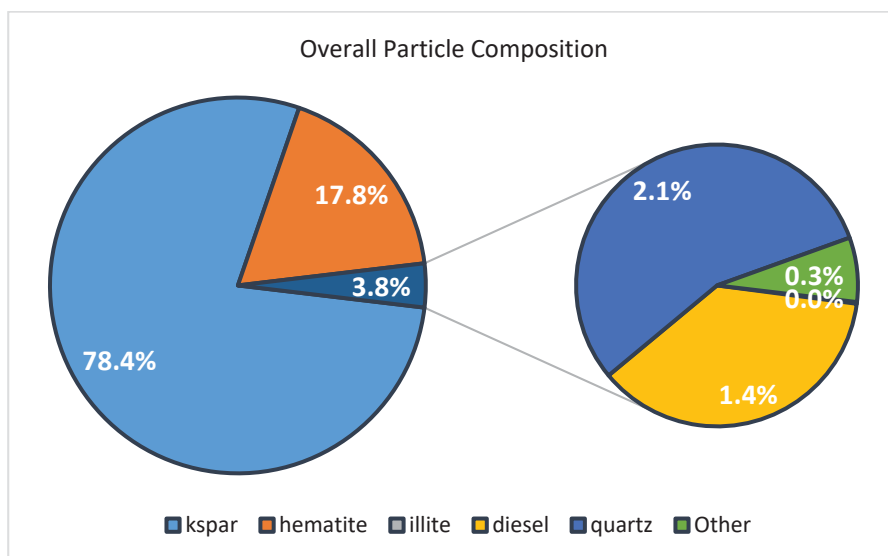

Figure 3. Pie chart of average results from three collection dates: June 25, 2015; July 27, 2015; September 24, 2015. The data show the percentage of results categorized by five subcategories of relatively

When broken down into the filter stages (**Figure 4**) for all sampling days, the largest (A) and smallest (D) particle sizes also have more composition attributed to other classes besides potassium feldspar. We note the limitations of the SEM to target individual particles of smaller size on stages B-D. In these smaller stages, each data point analyzed corresponds to elemental analysis of a cluster of particles both under and around the specific point. Since a high percentage of the particles sampled are likely to be feldspars, they would mask the signal given off by different particles.
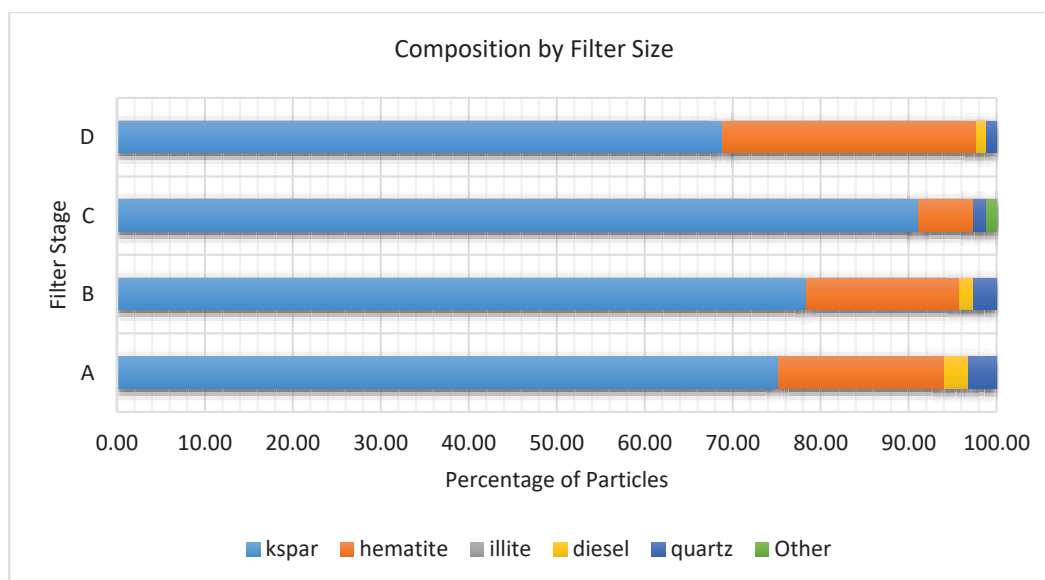
Figure 4. Average SEM-EDS results from three collection dates: 6/25/15; 7/27/15; 11/15. The data shows the distribution of the four subcategories of clays, and quartz, by filter stages.

DISCUSSION

Quartz makes up a small portion of the sampled particles emitted near a rock crusher in the sand mine, as determined by both the SEM-EDS analysis and the XRD analysis. The post-sampling weights in Table 3 show that there can be large amounts of particles deposited onto the filters, but that when those same filters are analyzed for quartz by XRD, it was not found above the experimental detection limits. The SEM-EDS analysis corresponds well to this showing that a majority of particles (over 75%) are classified as potassium feldspars. The only data from the XRD that quantified quartz at 16% of particle mass was on a date where the simultaneously sampled particles used in the SEM-EDS analysis only show roughly 6% of the largest particle stage was quartz. If we assume all Stage A particles had 6% quartz, on 9/24/15 that would correspond to 15 µg quartz, below the XRD detection limit, but on 11/15 this would correspond to 80 µg, which would have been above the detection limit. We consider these in rough agreement as the SEM-EDS analysis is not by mass and is semi-qualitative because not all particles are analyzed, and the analysis classifies by atom % instead of measurement by mass weight. The conclusions that the majority of particles sampled at the rock crusher in a sand mine also aligns with geological thin films studies of the sandstone formation, which assert that the large quartz spheres in the rock formation have a large diameter, much larger than would be airborne naturally, but the sandstone formation is held together by cements such as calcite, hematite and potassium feldspars.[22] These geological cements are smaller grain sizes within the rock formation and take up room in between the quartz spheres, and therefore are already closer to a size to become readily airborne (10 µm in diameter or less).

Weaknesses in this analysis are the exact identification of geologic materials from the SEM-EDS analysis. Our main goal was to identify quartz and be able to distinguish between it and other materials. Moreno *et al*.[19] applied an SEM-EDS technique to classify different types of silicates into different 5 different categories. These classification techniques were adopted and modified in this study because of the similar distribution of elements found in this study, which we used mainly to identify quartz (Moreno's Si-Felsic) and potassium feldspars (Moreno's AlSi-Felsic). The particles that we identify as hematite could be hematite combined with a feldspar, or could be contaminated with iron from mechanical wear of the rock crusher. There are few particles in our study containing magnesium and iron. We interpreted a large sulfur component to be diesel particulates, based on our analysis of diesel particles which show high carbon and sulfur peaks. The "other" category corresponds to particles that were unidentifiable, some of which contained large amounts of phosphorus, and trace amounts of transition metals such as titanium, molybdenum, and scandium. Even if the identification of non-quartz particles has higher uncertainty, our results with respect to the quartz content remain consistent with both the XRD and SEM-EDS analysis. At the ultra-fine stage, 0.25-0.50 µm, the most deeply respirable fraction of particles, the sample is primarily composed of feldspars and secondarily hematite, or iron-enhanced material (**Figure 4**). The percent of quartz particles in each filter stage was between 0.00 and 6.7% of the total particles.

SEM-EDS data show the particle sample consisted mostly of geologic materials instead of anthropogenic sources. The analyses obtained revealed that both fine and coarse ambient particles sampled were consistently silicates containing both aluminum and potassium, which leads us to assume they are potassium feldspars, although the origin of the feldspars could have come from previous weathering and deposition into the sandstone formation. This is to be expected because quartz and feldspar are the most common minerals in the Earth's crust. Feldspars and subsilic minerals are the most common parent material of aluminum.[23] This allows the conclusion that the weathering of feldspars resulted in clay materials present in the cement in the sandstone. In the samples collected, large amounts of the airborne feldspar are observed, which can be explained by the geology of sandstone. Odom[14, 24] discovered that fine-grained sandstone contained potassium feldspars. The cement is most likely represented by the feldspar category, specifically potassium feldspar, which holds the silica sand particles together. When the sandstone is crushed and fragmented at the sand-processing facility, the cement is destroyed, releasing an abundance of particulate feldspar into the air. Other cements that have been identified in these sandstone formations are calcite, quartz, hematite, goethite and silcrete.[22] Our results do not indicate a significant amount of dolomite, illite or calcite in the observed particles. Although there is a high silica content in the geological features of sandstone, small amounts of quartz particles are present in the airborne particle samples. In the geological formation most desirable for frac sand mining, the quartz grains are fine-to-course, meaning the spherical quartz grains in the formation have diameters ranging from 100-500 μm, larger by an order of magnitude from airborne particles. Because the mining process is to collect the silica sand particles, the processes are designed to abrade off the cement in the formation. Our results are consistent with the mechanical rock crushing producing smaller airborne particles consisting of geologic material found in the cement, rather than of quartz.

Observed differences between percent silica found on filters analyzed by XRD methods versus filters analyzed by SEM methods led to an investigation into possible interferences. Minerals commonly found in the mining sites were analyzed by XRD methods, and the locations of major peaks were compared to those found in a quartz sample. Calcite, kaolin, potassium feldspar, hematite, and muscovite were analyzed. Of these minerals, muscovite was the only one to present a significantly large peak in the same area as the major peak found in the quartz samples at about $2\theta = 26.8°$ (**Figure 5**).
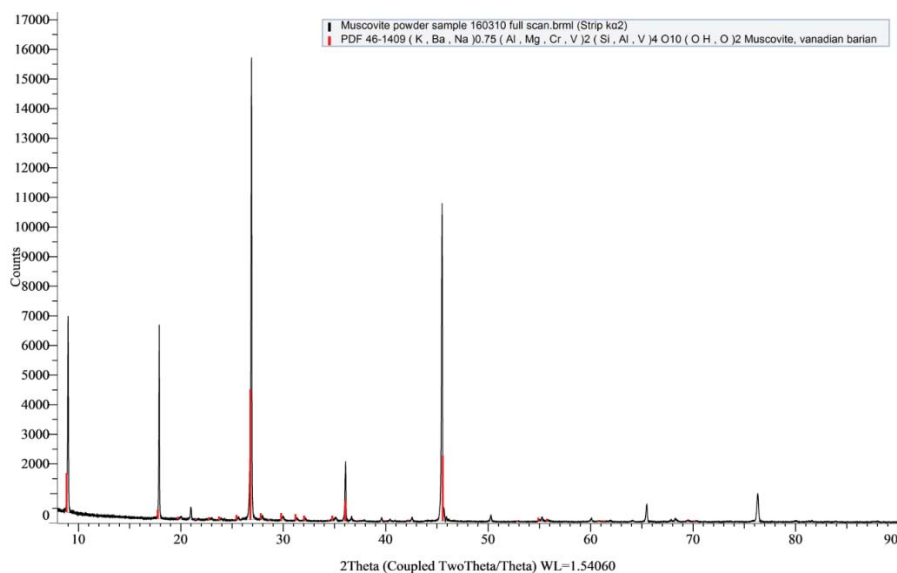

Figure 5. XRD pattern from a muscovite sample. Major peak occurs at $2\theta = 26.8°$.

If some of the material on the filters contained muscovite, a high bias for quartz could have resulted for the XRD analysis, which could explain some higher values for the % quartz on the filters as measured by XRD. A systematic error of higher of higher quartz by the XRD analysis could come from the feature shoulder shown in **Figure 1**, where the baseline is not level. That said, even with a higher peak area at this diffraction angle, few measurements were quantifiable above the detection limit for a majority of the samples. Because the SEM-EDS analysis was more qualitative, misidentification quartz in the smaller particle sizes could lead to an underestimation of quartz. The consistent result from both XRD and SEM-EDS analysis is that quartz is a small component (< 20%) of particulate matter from mining a rock formation that is 95% quartz.

A future study could employ sampling at different locations at the sand mining facility. The sampling strategy presented here was focused on an area where dust control measures were not taken at a location of active rock crushing. The emissions from this site could be representative of some particle-emitting processes in the mine (for example, when dynamite is used on outcrops), but would be less representative of other possible sources of ambient particles (for example, during the processing, sorting and storage of sand) that could arise from abrasion of quartz sand. Therefore, this study is not comprehensive for all ambient particles emitted in a sand mine.

CONCLUSIONS

The mass of particles typically collected on the filter samples during a 24-hour time period was about 2 mg, so a silica concentration of at least 32% would be needed to exceed the NIOSH Reference Exposure Level of 50 µg/m³ per 8 hours. Silica levels determined from our analyses are well below, with the maximum observed at 1.6 µg/m³ per 8 hours. Overexposure to dust particles can be hazardous to health, and in the case of the sand mines, exposure to respirable silica is the most harmful, but we find little evidence of high levels of respirable silica. The X-ray diffraction analysis shows that levels of respirable crystalline silica at the rock crusher are well below the REL. Most sample quartz masses were below the detection limit, and the samples that did surpass this value were much lower than the REL. SEM-EDS analysis supported this same conclusion, finding that only a small percentage of the particles were identified as quartz. Rather, particles were composed primarily of the cement, specifically potassium feldspar, from the rock formation.

REFERENCES

1. Davidson, C. I.; Phalen, R. F.; Solomon, P. A., (2005) Airborne particulate matter and human health: A review. *Aerosol Sci Technol* 39, 737–749.
2. Sanderson, W. T.; Steenland, K.; Deddens, J. A., (2000) Historical respirable quartz exposures of industrial sand workers: 1946-1996. *Am J Ind Med* 38, 389–398.
3. Walters, K.; Jacobson, J.; Kroening, Z.; Pierce, C., (2015) PM2.5 Airborne Particulates Near Frac Sand Operations. *J Environ Health* 78, 8–12.
4. Prengaman, K., Frac Sand Boom Creates Thousands of Jobs. WisconsinWatch.org: 2012. *http://wisconsinwatch.org/2012/08/sand-boom-creates-jobs/* (accessed Aug 2018)
5. Minnesota Department of Health (2013) Crystalline Silica Toxicological Summary. *http://www.health.state.mn.us/divs/eh/hazardous/topics/silica/silicaguidance.html* (accessed Aug 2018)
6. Borm, P. J. A.; Fowler, P.; Kirkland, D., (2018) An updated review of the genotoxicity of respirable crystalline silica. *Part Fibre Toxicol* 15, 17.
7. Ashley, K.; Fey O'Connor, P., (2016) *NIOSH Manual of Analytical Methods*. 5th ed.; National Institute for Occupational Safety and Health. *https://www.cdc.gov/niosh/docs/2003-154/chaps.html* (accessed Aug 2018)
8. Castranova, V.; Porter, D.; Millecchia, L.; Ma, J. Y. C.; Hubbs, A. F.; Teass, A., (2002) Effect of inhaled crystalline silica in a rat model: Time course of pulmonary reactions. *Mol Cell Biochem* 234, 177–184.
9. Hamilton, R. F.; Thakur, S. A.; Holian, A., (2008) Silica binding and toxicity in alveolar macrophages. *Free Radic Biol Med* 44, 1246–1258.
10. O.S.H.A., Respirable Crystalline Silica Standard 1926.1153. *https://www.osha.gov/laws-regs/regulations/standardnumber/1926/1926.1153* (accessed Aug 2018)
11. Shiraki, R.; Holmen, B. A., (2002) Airborne respirable silica near a sand and gravel facility in central California: XRD and elemental analysis to distinguish source and background quartz. *Environ Sci Technol* 36, 4956–4961.
12. Richards, J. R.; Brozell, T. T.; Rea, C.; Boraston, G.; Hayden, J., (2009) PM4 Crystalline Silica Emission Factors and Ambient Concentrations at Aggregate-Producing-Sources in California. *J Air Waste Manag Assoc* 59, 1287–1295.
13. Richards, J.; Brozell, T., (2015) Assessment of Community Exposure to Ambient Respirable Crystalline Silica near Frac Sand Processing Facilities. *Atmosphere* 6, 960–982.
14. Odom, I. E.; Wegrzyn, R. S.; Ostrom, M. E., (1978) Lithostratigraphy, petrology, and depositional environments of Jordan formation (Cambrian), Upper Mississippi Valley. *Am Assoc Pet Geol Bull* 62, 550–551.
15. Fliflet, R.; Poirier, J.; M.; Mahoney, J. B.; Syverson, K. (2016) Diagenetic History of Cambrian Sandstone Units in Western Wisconsin, *GSA Abstr Prog*: GSA Annual Meeting, Denver, CO.
16. Genga, A.; Baglivi, F.; Siciliano, M.; Siciliano, T.; Tepore, M.; Micocci, G.; Tortorella, C.; Aiello, D., (2012) SEM-EDS investigation on PM10 data collected in Central Italy: Principal Component Analysis and Hierarchical Cluster Analysis. *Chem Cent J* 6, 15.
17. Moroni, B.; Cappelletti, D.; Marmottini, F.; Scardazza, F.; Ferrero, L.; Bolzacchini, E., (2012) Integrated single particle-bulk chemical approach for the characterization of local and long range sources of particulate pollutants. *Atmos Environ* 50, 267–277.
18. Matassoni, L.; Pratesi, G.; Centioli, D.; Cadoni, F.; Lucarelli, F.; Nava, S.; Malesani, P., (2011) Saharan dust contribution

to PM10, PM2.5 and PM1 in urban and suburban areas of Rome: a comparison between single-particle SEM-EDS analysis and whole-sample PIXE analysis. *J Environ Monit* 13, 732–742.

19. Moreno, T.; Gibbons, W.; Jones, T.; Richards, R., (2003) The geology of ambient aerosols: characterising urban and rural/coastal silicate PM10-2.5 and PM2.5 using high-volume cascade collection and scanning electron microscopy. *Atmos Environ* 37, 4265–4276.

20. Gonzalez, L. T.; Rodriguez, F. E. L.; Sanchez-Dominguez, M.; Leyva-Porras, C.; Silva-Vidaurri, L. G.; Acuna-Askar, K.; Kharisov, B. I.; Chiu, J. F. V.; Barbosa, J. M. A., (2016) Chemical and morphological characterization of TSP and PM2.5 by SEM-EDS, XPS and XRD collected in the metropolitan area of Monterrey, Mexico. *Atmos Environ* 143, 249–260.

21. Radulescu, C.; Stihi, C.; Iordache, S.; Dunea, D.; Dulama, I. D., (2017) Characterization of Urban Atmospheric PM2.5 by ATR-FTIR, ICP-MS and SEM-EDS Techniques. *Rev Chim* 68, 805–810.

22. Runkel, T.; Syverson, K.; Steenberg, J.; Bendernagel, M.; Merchison, T.; Bauer, A.; Kent, A.; Thompson, M.; Stauffer, T.; Brown, B. (2012) In *Field Guidebook on the Silica Sand Resources of Western Wisconsin*, Conference on the Silica Sand Resources of Minnesota and Wisconsin, Brooklyn Park, MN.

23. Keller, W. D., (1964) The Origin of High-Alumina Clay Minerals - A Review. In *Clay and Clay Minerals*: Vol. 2, 129–151.

24. Odom, I. E., (1975) Feldspar-grain size relations in Cambrian arenites, Upper Mississippi Valley, *J Sediment Petrol* 45, 636–650.

ABOUT THE STUDENT AUTHORS:

Julie Zhang is an undergraduate student studying chemistry at the University of Wisconsin-Madison. She transferred there from UW-Eau Claire in Spring 2017 and expects to graduate in Fall 2018. Callie Fischer graduated in Spring 2018 with a degree in biochemistry/molecular biology and plans to attend medical school. Joe Oster graduated from UW-Eau Claire in Spring 2015 with a B.S. in Chemistry. Gabriel de Carvalho Chaves was a Brazilian Exchange student under the Brazilian Scientific Mobility Program and is currently a production engineering major at Pontifícia Universidade Católica de Minas Gerais with a graduation date in 2019. Rachel Mooney will graduate from UW-Eau Claire in Spring of 2019 with a degree in chemistry.

PRESS SUMMARY

Concern has arisen about levels of silica in ambient particles near frac sand mines in Northwestern Wisconsin. Exposure to particles containing silica can cause well-known adverse health effects. This study developed a parallel analysis using an X-ray diffraction (XRD) and scanning electron microscopy/energy-dispersive X-ray spectroscopy (SEM-EDS) analysis to test particles for silica in real air samples. Real air samples were collected at a frac sand site using a cascade impactor. A standard method to analyze silica on filters, NIOSH Method 7500, was followed that can detect respirable silica down to of 10-44 µg. The SEM-EDS used the elemental distribution found on the particles to assign parent geologic material. A majority (>80%) of the particles studied were found to be made up of substances other than silica, as determined by both methods.